Analyst

Accepted Manuscript

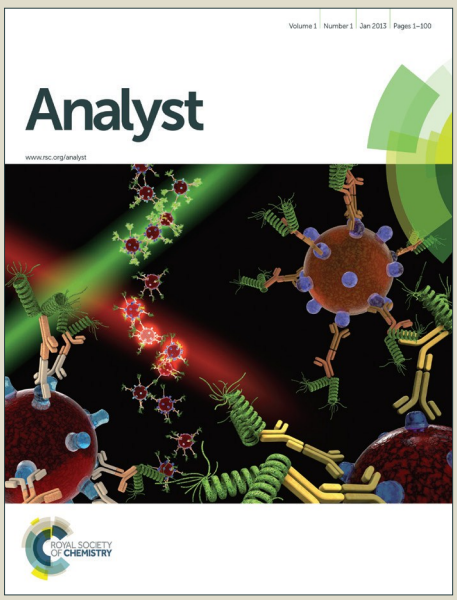

ROYAL SOCIETY OF CHEMISTRY

www.rsc.org/analyst

A non-PCR SPR Platform using RNase H to Detect MicroRNA 29a-3p from Throat Swabs of Human Subjects with Influenza A Virus H1N1 Infection

Jacky F.C. Loo [a,#], S.S. Wang [b,#], F. Peng [b,#], J.A. He [b], L. He [b], Y.C. Guo [b], D.Y. Gu [b,*], H.C. Kwok [c], S.Y. Wu [c], H.P. Ho [c] W.D. Xie [d] Y.H. Shao [e] S.K. Kong [a,*]

[a] Biochemistry Programme, School of Life Sciences, The Chinese University of Hong Kong, Room 609, Mong Man Wai Building, Shatin, NT, Hong Kong, China

[b] Shenzhen Entry-exit Inspection and Quarantine Bureau, Shenzhen 518033, China

[c] Center for Advanced Research in Photonics, Department of Electronic Engineering, The Chinese University of Hong Kong, Shatin, NT, Hong Kong, China

[d] Shenzhen Key Lab of Health Science and Technology, Division of Life Sciences & Health, Graduate School at Shenzhen, Tsinghua University, Shenzhen, China

[e] College of Optoelectronics Engineering, Key Laboratory of Optoelectronic Devices and Systems, Ministry of Education and Guangdong Province, Shenzhen Key Laboratory of Sensor Technology, Shenzhen University, Shenzhen 518060, China

[#] Co-First authors

[*] Corresponding author

Abstract

As in all RNA viruses, influenza viruses change and mutate constantly because their RNA polymerase has no proofreading ability. This poses a serious threat to public health nowadays. Also, traditional pathogen-based detection methods may not be able to report an infection from an unknown type or a subtype of virus if their nucleotide sequence is not known. Because of these, targeting host microRNA signatures may be an alternative to classify infections and distinguish types of pathogens as microRNAs are produced in human shortly after infection. Although this approach is in its infant stage, there is an urgent need to develop a rapid reporter assay for microRNA for disease control and prevention. As a proof of concept, we report here for the first time a non-PCR MARS (MicroRNA-RNase-SPR) assay to detect the microRNA miR-29a-3p from human subjects infected with influenza virus H1N1 by surface plasmon resonance (SPR). In our MARS assay, RNase H is employed to specifically hydrolyze the RNA probes immobilized on the gold surface where they hybridize with their cognate target, the cDNAs of miR-29a-3p from reverse transcription with stem-looped primers. After the digestion of the RNA probe by RNase H, the intact cDNA was released from the RNA-DNA hybrid and bound to a new RNA probe for another enzymatic reaction cycle to amplify signals. With assay optimization, the detection limit of our MARS assay for miR-29a-3p was found to be 1 nM and this new assay could be completed within 1 hour without thermal cycling. This non-PCR assay with high selectivity for mature microRNA provides a new platform for rapid disease diagnosis, quarantine and disease control.

Keywords

Surface plasmon resonance, RNase H, microRNA, influenza, miR-29a-3p

Abbreviations

LOD, limit of detection; LOQ, limit of quantitation; MARS, MicroRNA-RNase-SPR; miR, microRNA; RNase H, ribonuclease H; SPR, surface plasmon resonance

Highlight

A new non-PCR assay platform using RNase H to detect MicroRNA 29a-3p from patients' throat swabs with Influenza A virus H1N1 infection

Introduction

RNA is previously thought of as a simple decoding intermediate between DNA and protein for the transmission of genetic information. With more and more scientific research, a group of small protein noncoding RNAs discovered in 1993 is now known to engage in the regulation of gene expression [1]. This class of noncoding RNAs, known as microRNAs (miRs), is composed of a group of highly conserved small single-stranded RNAs (20-23 bases in length). They predominantly promote degradation of target messenger RNAs (mRNAs) or repress protein translation when their nucleotide sequence, after processing, exists in perfect or partial complementarity to their target transcripts at the 3'-untranslated region [2].

The human genome encodes over two thousand of distinct miRs (MicroRNA database: http://www.mirbase.org/) to regulate and fine-tune almost every biological function from cell proliferation, differentiation to cell death. In view of their important regulatory functions, it is not surprising that dysregulations in miRs are associated with various pathogenesis including diabetes [3], cardiovascular disorders [4], and cancer [5]. Also, miRs have been found to play important roles in influenza virus infection and host immune response [6,7].

Influenza viruses are enveloped RNA viruses and their genetic make-up mutates easily because their RNA polymerase has no proofreading ability. In view of the ever-changing genome in the influenza virus through gene mutation and also genetic reassortment between co-infecting viruses in host cells [8], it is difficult to develop a very updated reporter assay to identify an unknown strain of pathogen based on their RNA sequence. In this connection, using host miR as the biomarker to predict the likelihood of infection of unknown type of influenza virus may be another alternative.

Using miRs for diagnostic purpose, however, is challenging because of their intrinsic properties such as low abundance (e.g. 0.01% of the total RNA mass), short length (20-23 nucleotides in length) and

high homology in sequence among family members. For miRs sensing, real-time quantitative polymerase chain reaction (RT-qPCR), Northern blot analysis and microarray-based scanning are widely used among other detection techniques. However, each platform has its own advantages and disadvantages [9].

In this study, we introduced a new method called *MARS* (MicroRNA-RNase-SPR) assay using ribonuclease H (RNase H) and surface plasmon resonance (SPR) to sense a marker miR, miR-29a-3p, associated with influenza viral infection. RNase H is a sequence non-specific endonuclease found in the HIV-1 (human immunodeficiency virus type-1) and some other prokaryotes and eukaryotes. During HIV-1 infection, the RNA from the virus is reversibly transcribed into cDNA and the retroviral RNase H degrades the RNA in the RNA-DNA hybrid leaving the cDNA in host cells for viral replication [10,11].

It has been known for a while that mature miRs with 5'-end variations are generated from the primary miR transcripts by Drosha alternative processing [12]. To perform the MARS assay, a particular form of mature miR among other variants are first reversely transcribed into cDNA using stem-loop primers (Figure 1). Notably, the stem-loop at 5'-end is able to block the primers from annealing to other mature variants and the miR precursors (e.g. primary and pre-miRs), thus increasing the specificity and efficiency in the conversion of a distinct form of mature miR to cDNA [13].

On the SPR surface, miR probes with spacer at 3'-end and biotin at 5'-end are immobilized on the pre-cleaned gold surface by 3'-thiolated linkage via self-assembly. Unlike proteins, our miR probes and cDNAs are small (i.e. short length oligonucleotide) in nature, therefore association or dissociation does not change the SPR signals much. To increase SPR signals, streptavidins are added to the RNA probes through biotin-avidin interaction [14]. After washing, the surface is used to capture target cDNAs. RNase H is then introduced to the SPR chamber to digest the cDNA-bound RNA probes conjugated with streptavidin. Subsequently, the released cDNA binds to another miR probe for digestion. Cycle of reaction continues and most, if not all, the probes are cleaved and a change in SPR signals is generated (Figure 1).

As a proof of concept, synthetic *Homo sapiens* (hsa)-miR-29a-3p was used as the target miRs as it was found to be strongly associated with the influenza A H1N1 viral infection from human subjects crossing the Hong Kong-Shenzhen border (data not shown). In this study, we demonstrated for the first time that this new MARS method using RNase H and SPR is a sensitive, reliable and simple technique to detect the miR for influenza virus H1N1 infection with a detection limit at 1 nM and the process can be finished within 1 hour without using PCR thermal cycles.

Experimental Section

Materials and Reagents

Key reagents were obtained from the following sources. Chemicals for SPR sensing were purchased from Aladdin Reagent (Shanghai, China). Recombinant *E. coli* prokaryotic RNase H (molecular size: 18.5 kDa, original concentration of 60,000 U/mL) and RNase III (molecular size: 25.6 kDa, original concentration of 1,000 U/mL) were purchased from Takara Biotechnology (Dalian, China) and Life Technologies, respectively. Streptavidin was obtained from Bioss (China). All glasswares, pipette tips and solutions were autoclaved and cleaned with RNase AWAY Decontamination Reagent (Life Technologies) before use. The DNA and RNA sequences used in this study are summarized in Table 1.

Table 1. The DNA and RNA sequences used in this study (Capital = DNA, small letter = RNA)

Name	**Sequence (5' – 3')**
miR probe hsa-miR-29a-3p	(biotin)-uagcaccaucugaaaucgguuauuuuuuuu-(C6)-SH
miR probe hsa-miR-181-5p	(biotin)-aacauucaacgcugucggugaguuuuuuuuu-(C6)-SH
DNA probe hsa-miR-29a-3p	(biotin)-TAGCACCATCTGAAATCGGTTATTTTTTTT-(C6)-SH
cDNA of hsa-miR-29a-3p	TAACCGATTTCAGATGGTGCTA
cDNA of hsa-miR-181-5p	ACTCACCGACAGCGTTGAATGTT
H1N1 viral RNA forward primer	AACATGTTACCCAGGGCATTTCGC
H1N1 viral RNA reverse primer	GTGGTTGGGCCATGAGCTTTCTTT
H1N1 viral RNA molecular beacon probe	(VIC)-GAGGAACTGAGGGAGCAATTGAGTTCA-(TAMRA)

miR probe design and sensing surface preparation

The mature miR probes for the cDNA of hsa-miR-29a-3p (5'-taaccgatttcagatggtgcta-3') and miR-181-5p (5'-actcaccgacagcgttgaatgtt-3') were purchased from Takara Biotechnology (Dalian, China), with biotin at the 5'-end for streptavidin attachment for signal enhancement, and C-6 spacer at the 3'-end with thiol group for self-assembly onto the SPR gold surface. To prepare the sensing surface, 1 μM RNA probe in 0.2 μL sodium acetate buffer (5 mM sodium acetate at pH 7.8) was added on the SPR

gold sensing surface for 16 h at 4 ^{o}C for probe immobilization. Unbound region of the sensing surface was blocked with PEG 1000-SH for 2 h at room temperature (25 ^{o}C). After washing, the gold sensing surface was inserted into a SPR machine (GWC SPR imager II system) for sensing. Fifty μg/mL streptavidin or buffer was then introduced at a flow rate of 200 μL/min for 3 min. The sensing surface was then rinsed with the SPR binding buffer (100 mM KCl, 50 mM Tris, 10 mM $MgCl_2$, 10 mM DTT, pH 7.8) until a steady baseline was obtained where intensity fluctuation was smaller than 0.01.

SPR detection

Synthetic ssDNA mimicking the reversely transcribed cDNA from the hsa-miR-29a-3p was obtained from Takara Biotechnology (Dalian, China). One hundred μM stock solution was made using ddH_2O. ssDNA of various concentrations were then prepared in the SPR binding buffer and subjected to SPR detection at 25^{o}C. The ssDNA was injected into the SPR sensing chamber with a flow rate at 50 μL/min for 10 min. The chamber was then rinsed with buffer to obtain a steady baseline. RNase H (60 U/mL) was subsequently injected at a flow rate of 50 μL/min for 15 min, the gold surface was rinsed with buffer again to obtain a steady baseline. The intensity difference before and after RNase H addition was recorded.

Patient miR detection

Human samples were obtained from the Customs of Shenzhen, China. Ethics Approval was obtained from the Shenzhen Entry-exit Inspection and Quarantine Bureau, Shenzhen China and informed consent was obtained from patients and volunteers. Throat swabs containing secretions and infected cells, if any, from healthy controls or patients with influenza virus infection (strain A/China/04/2014 H1N1) were kept in sterile saline (0.85% NaCl) [15]. Total RNA was then extracted by TRIZOL reagent (Life Technologies) in a biosafety level-3 culture hood. Disease status of healthy donors and subjects suffered from H1N1 viral infection was confirmed by RT-PCR for the pathogenic H1N1 viral RNA using forward primer (5'-AACATGTTACCCAGGGCATTTCGC-3'), reverse primer (5'-GTGGTTGGGCCATGAGCTTTCTTT-3'), and molecular beacon probe 5'-(VIC)-GAGGAACTGAGGGAGCAATTGAGTTCA-(TAMRA)-3', with the following PCR cycling profile (95 ^{o}C 15

sec, 60 °C 45 sec for 40 cycles). For the preparation of miR, total RNA concentration was measured by Nanodrop (Thermo Scientific) to normalize the RNA amount for reverse transcription. Reverse transcription specific for the mature hsa-miR-29a-3p was then performed with Taqman miR reverse transcription kits (Life Technologies) according to manufacture protocols. Briefly, 10 ng total RNA was added into reverse transcription master mix containing reverse transcriptase, stem-loop primer and dNTP in a total volume of 20 μL and reverse transcription was performed at 42°C for 30 min. Subsequently, the original RNA was denatured by heat at 95°C for 10 min, then cool to 25°C. The cDNA was then subjected to SPR detection as described above. RT-PCR, in terms of Ct (threshold cycle) value, was performed to confirm the relative fold change difference of the miR-29a-3p cDNA between healthy donors and H1N1 patients. Ct value is the PCR cycle number that gives a detectable amplification signal (threshold) from reactions. The lower the Ct value, the more is the initial cDNA copies for PCR amplification.

Statistical analysis

Results are mean±SD from at least three independent assays unless otherwise stated. All of the experimental results were analyzed by Student's *t*-test, *p*-values less than 0.05 were considered statistically significant.

Results

miR quantitation and signal enhancement by biotin-streptavidin in the MARS assay

SPR detection is sensitive to small changes in the refractive index of materials at the interface between a thin gold film and a bulk solution [16,17]. Although it is a label-free techique that quantifies biomolecular interactions, binding of streptavidin to the biotinlated RNA probes immobilized on gold surface was employed in our study to amplify the SPR signals and enhance the SPR sensing sensitivity.

As shown in a typical set of sensorgrams in Figure 2, hybridization between the DNAs of known concntrations and its corresponding RNA probe with streptavidin showed a stronger increase in the SPR signals (Figure 2A) than that without streptavidin (Figure 2B). Obviously, our data show that streptavidin did not interfere with the binding of DNA to the RNA probes (Figure 2A). For the signals generated by enzyme digestion, a deeper decrease in the SPR signals (signal change ~10-fold) was obtained from the probes with streptavidin 100 sec after the addition of RNase H (Figure 2C) when comapred to that without streptavidin (Figure 2D). Experiments were repeated thrice and data extracted from these experiemnts. As can be seen in Figure 2E, the SPR readouts started to show a significant change from the DNA samples 20 nM onwards. These results indicate that using biotin-streptavidin in our platform could significantly improve the signal-to-nosie ratio and assay sensitivity.

Next, we tried to establish the limit of detection (LOD) for our MARS plateform. According to the definition of LOD (the lowest concentration of a substance that can be distinguished from blank without that substance), LOD was calculated as signal at blank plus three times of standard deviation followed the recommendation by the IUPAC (International Union of Pure and Applied Chemistry), i.e. 0.0036 + (3 x 0.0003) = 0.0045 intensity level, corresponding to a concentration below 1 nM (Fig.2F). For quantitative detection, we used limit of quantitation (LOQ, the limit at which one can differentiate the difference between two different values), which was defined as signal at blank plus ten times of standard deviation, i.e. 0.0036 + (10 x 0.0003) = 0.0066. As RNase H generates a negative SPR signal after digesting the probes, the LOQ (-0.0066) will fall within the range 0 nM (0.0036) to 1 nM (-0.0491)

(Fig.2F). It appears that the detection limit of our MARS platform could reach <1 nM for quantitation. For the relationship between SPR signal and miR concentration, there is a negative relationship between the data, i.e. a negative slope of -0.0026 from 10-100 nM of miR without using biotin-streptavidin, while -0.0076 from 1-70 nM and -0.073 from 70-100 nM with the biotin-streptavidin enhancement (Fig. 2E). The larger magnitude of the negative slope indicates that the SPR signal changes more dramatically when the miR concentration is larger than 70 nM in the presence of biotin-streptavidin.

Specificity in the MARS assay

Specificity is another important concern for our MARS sensors. Specificity is evaluated by real-time SPR imaging based on hybridization between immobilized probes and testing ligands, and subsequent digestion of the RNA probes on the gold SPR surface by the RNase H. As can be seen in Figure 3, single stranded DNA (ssDNA) probe for miR-29a-3p and miR probes for hsa-miR-29a-3p and hsa-miR-181-5p were immobilized on different sensing areas of one sensor chip. Subsequently, cDNAs of hsa-miR-29a-3p and hsa-miR-181-5p, RNase H and buffer were added at the time points (i-v) as indicated.

Panel A in Figure 3 shows a sensorgram for the ssRNA probe miR-29a-3p. As can be seen, a small increase in signal after the injection of cDNA of miR-29a-3p at time point (i) was observed showing annealing of the two strands. An abrupt decrease in the SPR signals was obtained immediately after the addition of RNase H at time point (ii) indicating an enzymatic digestion of the RNA pobes from the RNA-DNA hybrid by RNase H. Further injections of miR-181-5p, RNase H and buffer at time points (iii)-(v) did not change the baseline indicating the binding specificty and complete digestion of the probes on the sensor chip.

Panel B depicts the sensorgram for the ssRNA probe miR-181-5p. The first addition of cDNA of miR-29a-3p at time point (i) did not generate any increase in response, confirming the specificity of binding. No change was seen when RNase H was added at the time point II again showing the requirement of the presence of DNA-RNA hybrid for the enzymatic hydrolysis. As expected, injection of cDNA of miR-181a-5p at time point (iii) increased the SPR signals while injection of RNase H at time

point (iv) decreased the SPR signals in a way similar to that in Panel A, confirming again the specificity of binding and digestion (Figure 3).

In Panel C, miR-29a-3p cDNA was likewise added at time point (i) for the ssDNA probe miR-29a-3p and this challenge produced a small rise in the SPR signals indicating hybridization between the ssDNA probe and its target DNA. The later addition of RNase H at time point (ii) and cDNA of miR-181a-5p at time point (iii) and RNase H again at time point (iv) did not generate any change in response suggesting that RNase H could not digest the DNA probe in the DNA-DNA hybrid.

Panel D in Figure 3 serves as a control and additions of cDNAs of miR-29a-3p and miR-181a-5p, and RNase H did not produce any increase or decrease in signals as the RNA probe had been omitted and the sensing gold surface had been saturated with the blocker PEG 1000-SH. For easy comparison, results in Panels A-D, signals from one single chip in fact, were merged together and shown in Panel E.

In Panels F and G (Figure 3), we repeated the assay using RNase III instead of RNase H with the cDNA of miR-29a-3p (Panel F) or ssRNA of miR-29a-3p (Panel G) on the sensing chip of the same configuration as mentioned in Panels A-E. RNase III is an enzyme that digests dsRNA to dsRNA fragments of ~12 bp long but not other formats such as the dsDNA or RNA-DNA hybrids [18]. For clear comparison, we set the sensorgrams from the 4 regions of chip to the same baseline no matter if a hybridization had occurred or not. RNase III was then introduced into the system. Maybe due to a large amount of the RNase III used, (although only 5 U/mL had been used in the assay (vs. 60 U/mL of RNase H)), an immediate increase in the SPR intensity was observed in both panels indicating the association of the enzyme on the sensing surface. As can be seen in Panel F with the in-flow cDNA, no signal decrease was observed and all four time-course tracings were more or less the same. These indicate that the RNase III did not cleave any probes on the SPR surface since no dsRNA was present on the sensing surface.

On the contrary, a significant decrease in SPR signal was obtained only from the region with the cognate RNA probe in Panel G with the in-flow ssRNA. No such change was found from the region

immobilized with the DNA probe with complimentary sequence, not to mention the blank control nor the unrelated ssRNA probe. These results indicate the specific dsRNA cleavage by the RNase III and also the functionality of the RNase III we used in Panel F. Taken together, our results demonstrate the specificity between the precise hybridization of probes to their corresponding targets and the specific enzyme activity from RNase H but not others such as the RNase III contamination in the MARS assay.

Using the MARS assay to detect the miR-29a-3p from the patients infected with H1N1

To demonstrate the utility of our new detection platform, we utilized a pilot samples from 20 patients with H1N1 influenza virus infection collected during the seasonal influenza period in April 2014. Disease status of subjects was first confirmed by the RT-qPCR with specific primers against the H1N1 marker RNA as described in 'Experimental Section'. As shown in Figure 4A, signals from the healthy subjects remained at background level until the end of the experiment. On the contrary, remarkable increase in fluorescent signals was obtained from patient sample after 25 cycles suggesting that the samples were H1N1 positive.

Next, RNAs were extracted from the throat swabs of subjects with influenza virus H1N1 infection, and that of healthy donors for comparison. For the detection of miR, mature hsa-miR-29a-3p was first reversely transcribed into cDNA with stem-loop primers. As mentioned before, this method can pick up the mature miR selectively and effectively, and eliminate the pre-mature miR or other isoforms generated by alternative Drosha processing [12]. Total RNA (10 ng) from each individual was subject to reverse transcription and analysized via both MARS assay and real-time qPCR.

As can be seen from the MARS assay (Figure 4B), patient samples showed a bigger change for miR-29a-3p. With the information from standard curves, the miR-29a-3p level from patients and healthy subjects were found to be 6.8 ± 2.4 and 17.8 ± 2.4 nM respectively. The same preparations were then re-examined using RT-qPCR assay. Again, the miR-29a-3p was found to be downgulated by a Ct difference of 1.92 from the disease samples (Figure 4C). For these results, it is noteworthy that only 30 minutes (i.e. 15 min for cDNA-RNA hybridization and 15 min for RNase H action) were required to complete the MARS assay while more than 3 hours were needed for the RT-qPCR.

Discussion

Influenza viruses are the enveloped RNA virus belonging to the *Orthomyxoviridae* family. They remain one of the major public health threats of this centry [19]. With the antigenic drift by RNA polymerase errors and antigenic shift by gene reassortment, new strains of pathogen may appear which are not recognized by human defence system after vaccination and may thus cause epidemics and pandemics [8].

Although still in its infant stage, global miR profiling will potentially identify miR signatures as the biomarkers of influenza [20]. In this study, we reported a new and rapid diagnostic method using RNase H to detect host miR. Using conventional RT-qPCR and our MARS assay, we found miR-29a-3p was down-regulated in the throat swabs of the subjects infected with influenza A virus H1N1 (Figure 4). In the miR-29 family, there are three members, namely, miR-29a, miR-29b, and miR-29c. In particular, miR-29 was found to suppress the host immune response by targeting interferon-gamma in mouse model [21]. Moreover, expression of miR-29c, associated with NF-κB activity, significantly inhibited the production of several anti-viral and pro-inflammatory cytokines in the H1N1-infected *in vitro* model [22]. As the alignment score between the miR-29a and miR-29c is high, it is likely that the down-regulated level of miR-29a found in the throat swabs from the subjects with H1N1 infection may indicate a protective response generated from host against the H1N1.

In our MARS system, we used RNase H to digest the RNA probes on the gold SPR surface and the LOD was found to be 1 nM. Practically, the stability of our RNA probe was found surprisingly high. Storage of the probes at 4 ^{o}C up to two weeks did not affect the efficiency on cDNA binding and SPR signals (Supplementary Figure 1). This may be due to the fact that the sequence of our probe is indeed a miR, which is highly stable. Results from literature indicate that miR remained intact even in the formalin-fixed paraffin-embedded tissues [23].

For the action of RNase H, it requires a substrate with an RNA stretch containing at least four ribonucleotides in a RNA-DNA hybrid. If the RNA-DNA hydrid has only 4 bases, the RNase H digestion

starts from the fourth nucleotide from the 5'-end [24,25]. It can be imagined that the longer the RNA-DNA hybrid length, the more the RNA site can be cleaved by the RNase H. To meet this requirement, our miR-29a-3p probe was 100% RNA and contained a total of 22 bases which provides multiple sites for hydrolysis. Also, this design reduces the possible steric hindrance problem from streptavidin thereby improving the assay sensitivity and detection limit.

Experimentally, we found that 200 μL out of 5 mL of throat swab saline yielded more than 100 ng RNA which was sufficient for SPR sensing. Taking the volume of cDNA injected (500 μL) into the account, the detection limit of our MARS assay was 500 fmol in our experimental condition (60 U/mL RNase H 15 min action, 25 ^{o}C). It matched with other SPR detection methods with a detection limit at femtomole level [26,27]. Although the detection limit of some other methods such as RT-qPCR reaches fM level, they took a much longer time for sensing [13].

Unlike RT-qPCR using beta-actin or GAPDH for normalization, we could not identify a suitable house-keeping miR for data normalization. In fact, there are findings showing that different tissue has different endogenous miR references [28]. To solve this problem, we normalized our samples by the RNA input amount. In this connection, more work is needed to identify a suitable miR reference for normalization for throat swab samples.

In our study, a 2 x 2 array and SPR imaging were employed to test the assay specificity (Figure 3). It is anticipated that a more high throughput MARS microarray (n x n) can be used to detect the miR signatures for influenza if more information from research (e.g. miR control for normalization) and the global miR profiling are available. Once the database is provisioned, the pattern of infection-induced miR change can be used as a barcode for disease identification.

Conclusions

We have demonstrated here for the first time that our new MARS assay using RNase H and specific RNA probe is a selective, simple (using one temperature for signal generation), sensitive (LOD at 1 nM) and fast (process can be completed within 1 h) method to screen miR by SPR. Our MARS assay is

only a starting point and we anticipate that more assay formats will be developed along this direction. To conclude, our MARS assay is a robust approach that might assist public health agencies in the next influenza pandemic to control and prevent the disease.

Acknowledgement

This work is supported by an ITF Grant (GHX/002/12SZ), CRF grant (CUHK1/CRF/12G), AoE (AoE/P-0/12) funding from the Hong Kong Special Administrative Region and the fund (SGLH20121008144756945) from Shenzhen, China.

Author contributions statement

SKK, DYG, HPH, WDX and YHS designed the study and obtained funding for the project. SYW and HCK developed the methodology and fine-tuned the software and hardware for SPR detection. JAH, LH and YCG collected human samples, identified the target for detection, designed the probes for tests. JFCL, SSW and FP prepared reagents, performed experiments, collected data and ran the first level analysis including statistical calculations. JFCL and SKK prepared figures and wrote the manuscript. SKK, DYG, HPH, WDX and YHS critically discussed and revised the article for paper submission.

References

1. Bartel DP. MicroRNAs: genomics, biogenesis, mechanism, and function. Cell. 2004 Jan 23;116(2):281-97.

2. Ha M, Kim VN. Regulation of microRNA biogenesis. Nat Rev Mol Cell Biol. 2014 Aug;15(8):509-24.

3. Singer RA, Arnes L, Sussel L. Noncoding RNAs in β cell biology. Curr Opin Endocrinol Diabetes Obes. 2015, 22:77–85.

4. Arunachalam G, Upadhyay R, Ding H, Triggle CR. MicroRNA signature and cardiovascular dysfunction. J Cardiovasc Pharmacol. 2014 Nov 10. [Epub ahead of print]

5. Sita-Lumsden A, Dart DA, Waxman J, Bevan CL. Circulating microRNAs as potential new biomarkers for prostate cancer. Br J Cancer. 2013 May 28;108(10):1925-30.

6. Tambyah PA, Sepramaniam S, Mohamed Ali J, Chai SC, Swaminathan P, Armugam A, Jeyaseelan K. microRNAs in circulation are altered in response to influenza A virus infection in humans. PLoS One. 2013 Oct 7;8(10):e76811.

7. Zhang X, Dong C, Sun X, Li Z, Zhang M, Guan Z, Duan M. Induction of the cellular miR-29c by influenza virus inhibits the innate immune response through protection of A20 mRNA. Biochem Biophys Res Commun. 2014 Jul 18;450(1):755-61

8. Szewczyk B, Bieńkowska-Szewczyk K, Król E. Introduction to molecular biology of influenza a viruses. Acta Biochim Pol. 2014;61(3):397-401.

9. Tian T, Wang J, Zhou X. A review: microRNA detection methods. Org Biomol Chem. 2015 Feb 10;13(8):2226-38.

10. Moelling K. Targeting the retroviral ribonuclease H by rational drug design. AIDS. 2012 Oct 23;26(16):1983-93.

11. Cerritelli SM, Crouch RJ. Ribonuclease H: the enzymes in eukaryotes. FEBS J. 2009 Mar;276(6):1494-505.

12. Wu H, Ye C, Ramirez D, Manjunath N. Alternative processing of primary microRNA transcripts by Drosha generates 5' end variation of mature microRNA. PLoS One. 2009 Oct 27;4(10):e7566.

13. Chen C, Ridzon DA, Broomer AJ, Zhou Z, Lee DH, Nguyen JT, Barbisin M, Xu NL, Mahuvakar VR, Andersen MR, Lao KQ, Livak KJ, Guegler KJ. Real-time quantification of microRNAs by stem-loop RT-PCR. Nucleic Acids Res. 2005 Nov 27;33(20):e179.

14. Zhang, D., Yan, Y., Cheng, W., Zhang, W., Li, Y., Ju, H., Ding, S. Streptavidin-enhanced surface plasmon resonance biosensor for highly sensitive and specific detection of microRNA. *Microchim Acta* (2013) 180:397–403.

15. WHO guidelines for the collection of human specimens for laboratory diagnosis of avian influenza infection

(http://www.who.int/influenza/human_animal_interface/virology_laboratories_and_vaccines/guidelines_collection_h5n1_humans/en/)

16. Yuan W, Ho HP, Suen YK, Kong SK, Lin C. Improving the sensitivity limit of surface plasmon resonance biosensors by detecting mixed interference signals. Appl Opt. 2007 Nov 20;46(33):8068-73.
17. Ng SP, Loo FC, Wu SY, Kong SK, Wu CM, Ho HP. Common-path spectral interferometry with temporal carrier for highly sensitive surface plasmon resonance sensing. Opt Express. 2013 Aug 26;21(17):20268-73.
18. Amarasinghe AK, Calin-Jageman I, Harmouch A, Sun W, Nicholson AW. Escherichia coli ribonuclease III: affinity purification of hexahistidine-tagged enzyme and assays for substrate binding and cleavage. Methods Enzymology 2001 Dec; 342:143–158.
19. Mathews JD, Chesson JM, McCaw JM, McVernon J. Understanding influenza transmission, immunity and pandemic threats. Influenza Other Respir Viruses. 2009 Jul;3(4):143-9.
20. Tambyah PA, Sepramaniam S, Mohamed Ali J, Chai SC, Swaminathan P, Armugam A, Jeyaseelan K. microRNAs in circulation are altered in response to influenza A virus infection in humans. PLoS One. 2013 Oct 7;8(10):e76811.
21. Ma F, Xu S, Liu X, Zhang Q, Xu X, Liu M, Hua M, Li N, Yao H, Cao X.The microRNA miR-29 controls innate and adaptive immune responses to intracellular bacterial infection by targeting interferon-gamma. Nat. Immunol. 12 (2011) 861–869.
22. Zhang X, Dong C, Sun X, Li Z, Zhang M, Guan Z, Duan M. Induction of the cellular miR-29c by influenza virus inhibits the innate immune response through protection of A20 mRNA. Biochem Biophys Res Commun. 2014 Jul 18;450(1):755-61.
23. Xi Y, Nakajima G, Gavin E, Morris CG, Kudo K, Hayashi K, Ju J. Systematic analysis of microRNA expression of RNA extracted from fresh frozen and formalin-fixed paraffin-embedded samples. RNA. 2007 Oct;13(10):1668-74.
24. Shibahara S, Mukai S, Nishihara T, Inoue H, Ohtsuka E, Morisawa H. Site-directed cleavage of RNA. Nucleic Acids Res. 1987 Jun 11;15(11):4403-15.
25. Inoue H, Hayase Y, Iwai S, Ohtsuka E. Sequence-dependent hydrolysis of RNA using modified oligonucleotide splints and RNase H. FEBS Lett. 1987 May 11;215(2):327-30.
26. Sípová H, Zhang S, Dudley AM, Galas D, Wang K, Homola J. Surface plasmon resonance biosensor for rapid label-free detection of microribonucleic acid at subfemtomole level. Anal Chem. 2010 Dec 15;82(24):10110-5.
27. Fang S, Lee HJ, Wark AW, Corn RM. Attomole microarray detection of microRNAs by nanoparticle-amplified SPR imaging measurements of surface polyadenylation reactions. J Am Chem Soc. 2006 Nov 1;128(43):14044-6.

28. Technical Notes: Endogenous Controls for Real-Time Quantitation of miRNA Using TaqMan® MicroRNA Assays. (http://www3.appliedbiosystems.com/cms/groups/mcb_marketing/documents/generaldocuments/cms_044972.pdf)

Figure legends

Figure 1. The MARS assay showing the design and workflow for miR sensing. First, mature miR but not the miR precursors is converted into cDNA by stem-loop primers (top A to D). On the gold SPR surface (bottom), biotinylated-miR probes (single stranded RNA molecules) with spacer C6 are immobilized through thio-linkage. After washing, unbound region on the sensing surface is saturated with blocker PEG. Streptavidins are then added to bind to the immobilized miR probes. The SPR surface is now ready to capture target cDNAs based on complementary base pair hybridization. Such binding generates RNA-cDNA hybrids and causes an increase in SPR signal. Subsequently, RNase H is introduced to digest the RNA probes. After digestion, the cDNAs remain intact and bind to new miR probes waiting for further RNase H digestion. Cycle of reaction continues and SPR signal is generated.

Figure 2. Quantification of the target cDNA. DNA of known concentrations are added to the SPR sensing chamber to hybridize with the RNA probes with (**A**) or without (**B**) streptavidin and the SPR signals were recorded. Subsequently, RNase H (60 U/mL) was introduced to digest the RNA probes with (**C**) or without (**D**) streptavidin (SA), concentrations of DNA in tracings in A and B (from top to bottom) and C and D (from bottom to top): 100, 70, 50, 20, 10, 1 (A and C only), 0 nM. Standard curves with or without streptavidin in SPR intensity for RNase H treatment against DNA concentration were plotted from the data obtained in A to D (**E**). Results are mean ± SEM from 3 independent measurements, * $p<0.05$ compared with corresponding blank control with or without streptavidin. (**F**) The normal distribution of SPR change for the measurement of cDNA from miR using the MARS sensor. The SPR change data density (bar) with normal distribution fitting (smooth curve) for detecting the LOD of DNA at the concentration of 1 nM (red) as a comparison to buffer alone (blue).

Figure 3. Specificity of miR probe on target cDNA detection. The miR probes (ssRNA) hsa-miR-29a-3p (blue), ssDNA probe miR-29a-3p (red), hsa-miR-181-5p (green) or PEG only (purple) were immobilized on the SPR sensing surface of a single chip in the area as indicated. The cDNA of hsa-miR-29a-3p and hsa-miR-181-5p (100 nM), and RNase H (60 U/mL) were added at the time points as indicated. Panel

(**A**): SPR surface immobilized with ssRNA miR probe miR-29a-3p; Panel (**B**): ssRNA miR probe miR-181-5p; Panel (**C**): ssDNA probe miR-29a-3p, Panel (**D**): blank control and Panel (**E**): merged diagram. The signal change was compared with the blank control (purple) to reveal the specificity for probe-target binding and RNase H action on RNA-DNA and DNA-DNA hybrid. Single-stranded cDNA (**F**) or single-stranded RNA (**G**) of hsa-miR-29a-3p (100 nM) was introduced to the chip with the same configuration as mentioned above for hybridization (hybridization data not shown). After establishing a baseline, RNase III (5 U/mL) was added and SPR signal intensity detected. At the end of the experiment, the sensor chip was washed with buffer until a new baseline was made available.

Figure 4. Screening patient samples by MARS assay. Total RNA from human subject's throat swabs was extracted and transcribed into cDNA. RNA markers were screened for the presence of influenza A virus H1N1 via real time qPCR (Forward primer 5'-AACATGTTACCCAGGGCATTTCGC-3', Reverse Primer 5'-GTGGTTGGGCCATGAGCTTTCTTT-3', Probe 5'-(VIC) GAGGAACTGAGGGAGCAATTGAGTTCAG (TAMRA)-3', PCR Cycling profile 95 ^{o}C 15 sec, 60 ^{o}C 45 sec for 40 cycles) to confirm infection (**A**). The cDNA corresponding to healthy control and H1N1-infected sample was added to the SPR sensing surface for miR-29a-3p detection. With the information from the standard curve, concentration of the miR was determined. Results are mean ± SEM from three independent measurements (**B**). To validate the relative expression level of miR, RT-qPCR was conducted and deltaCt calculated. Results are mean ± SD from 20 samples. The low deltaCt value shows a high yield of cDNA in the sample in the RT-qPCR (**C**).

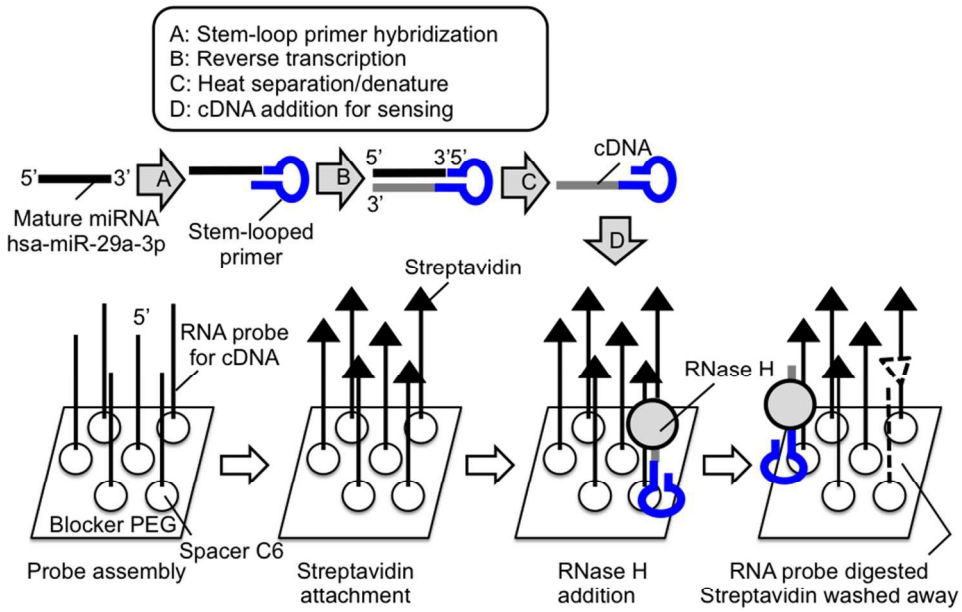

Figure 1

352x264mm (72 x 72 DPI)

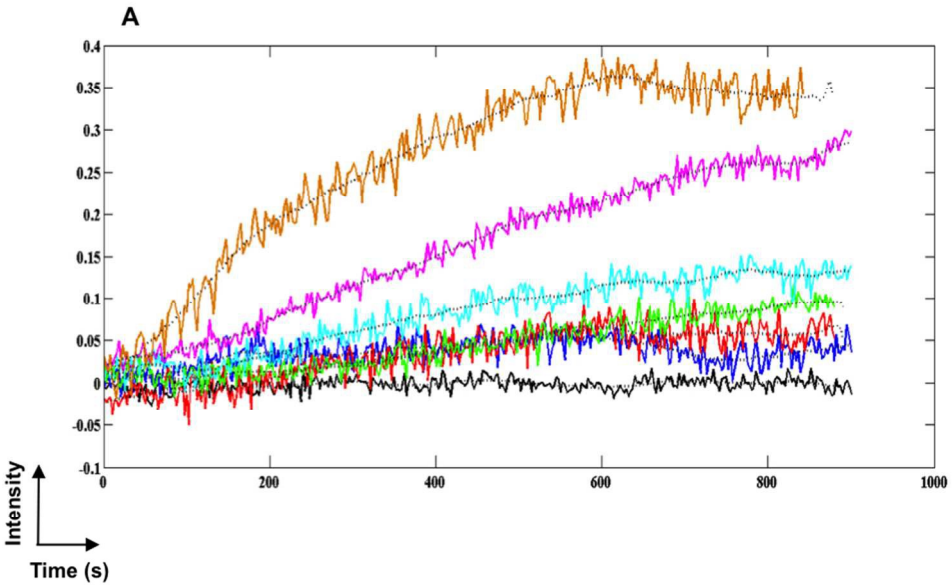

Figure 2

352x264mm (72 x 72 DPI)

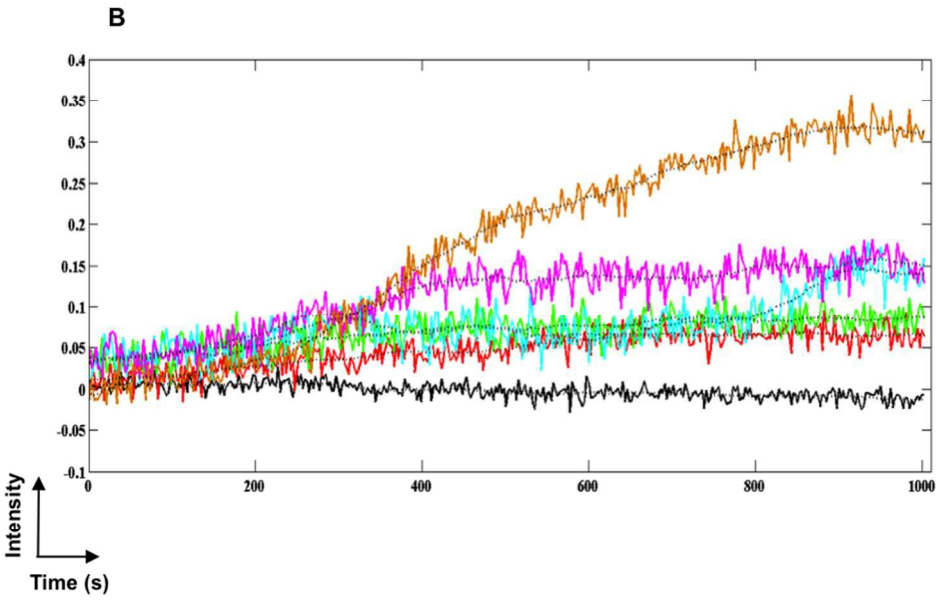

Figure 2

352x264mm (72 x 72 DPI)

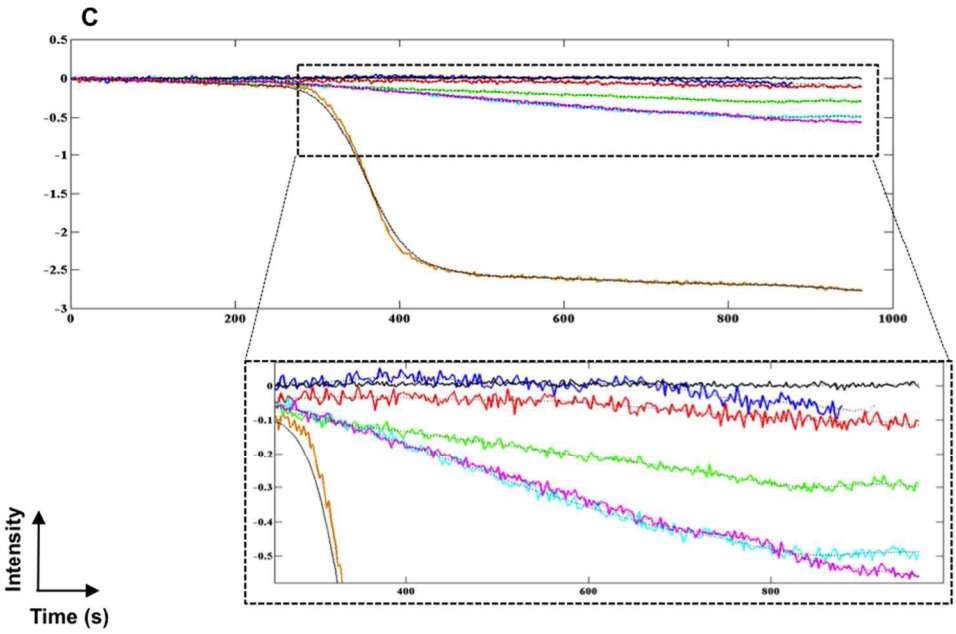

Figure 2

352x264mm (72 x 72 DPI)

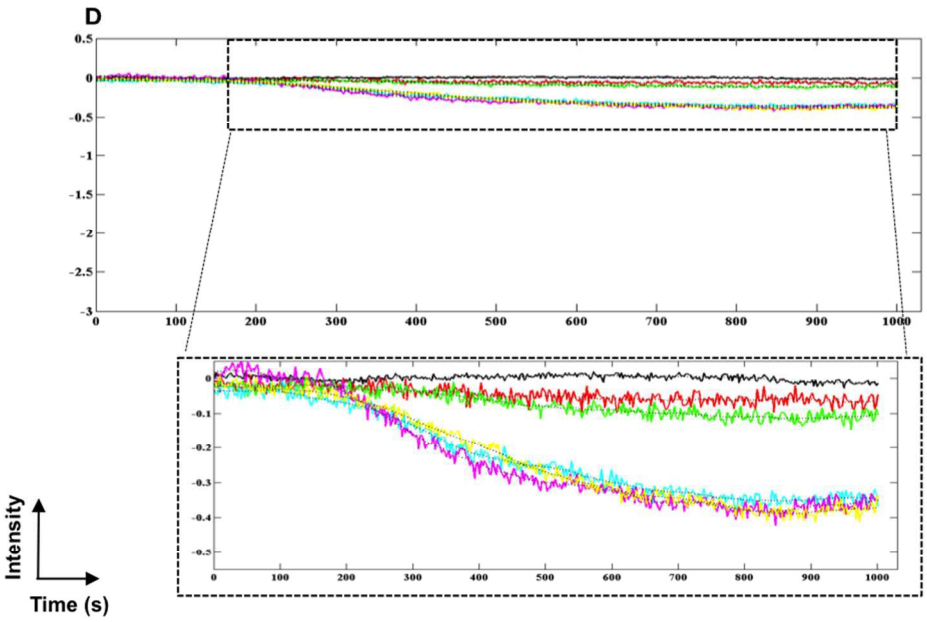

Figure 2

352x264mm (72 x 72 DPI)

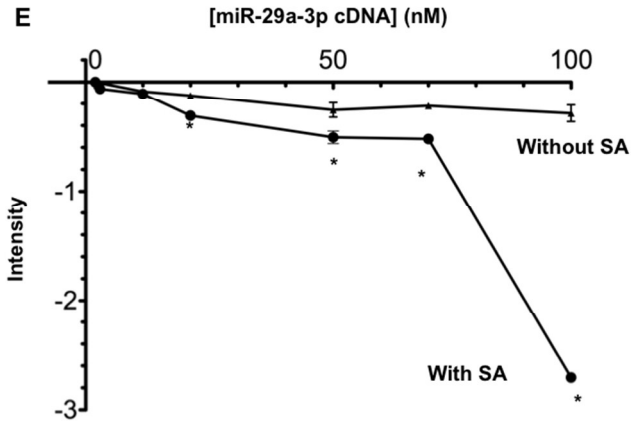

Figure 2

352x264mm (72 x 72 DPI)

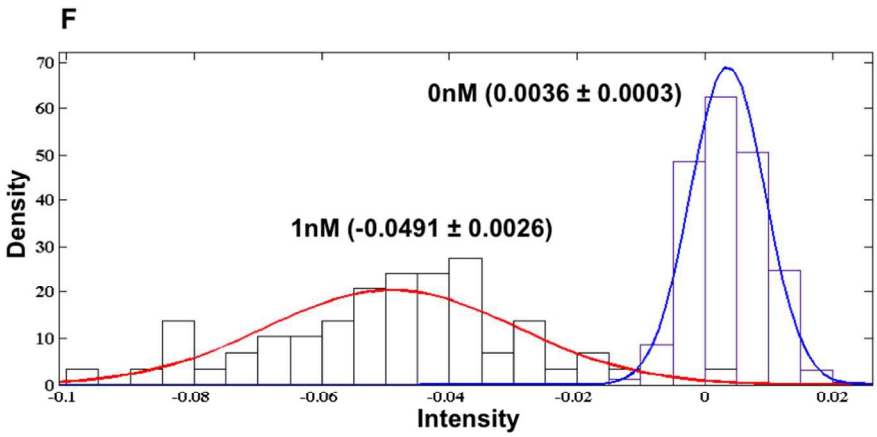

Figure 2

352x264mm (72 x 72 DPI)

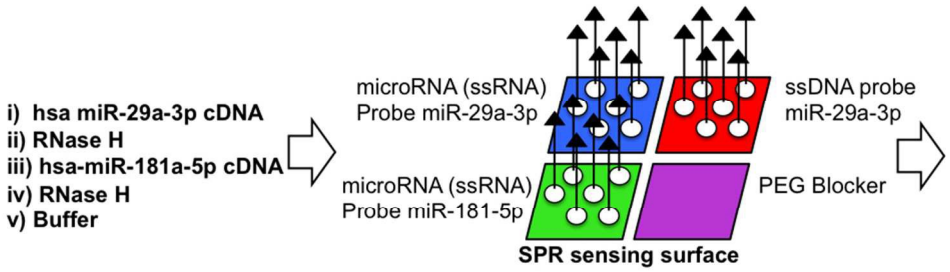

Figure 3

352x264mm (72 x 72 DPI)

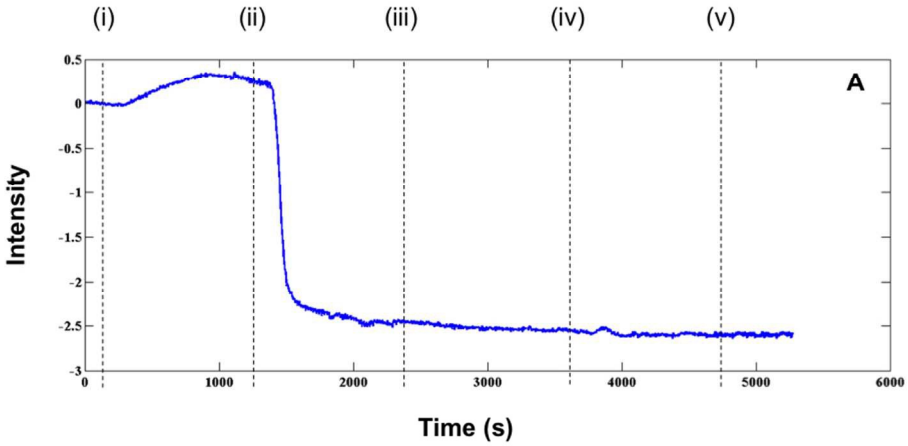

Figure 3

352x264mm (72 x 72 DPI)

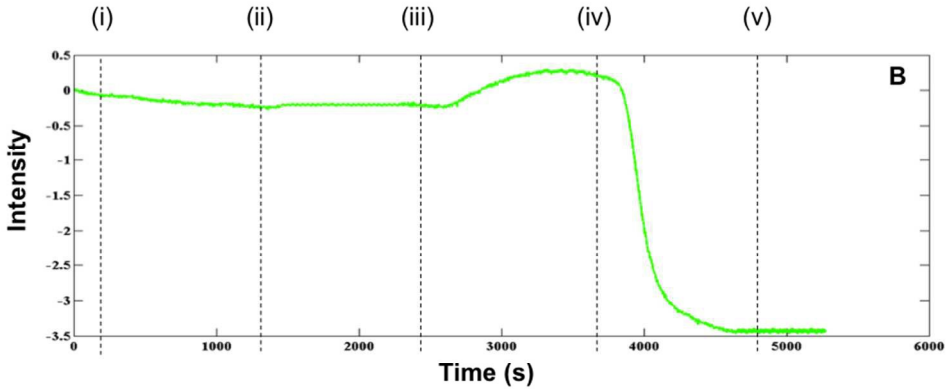

Figure 3

352x264mm (72 x 72 DPI)

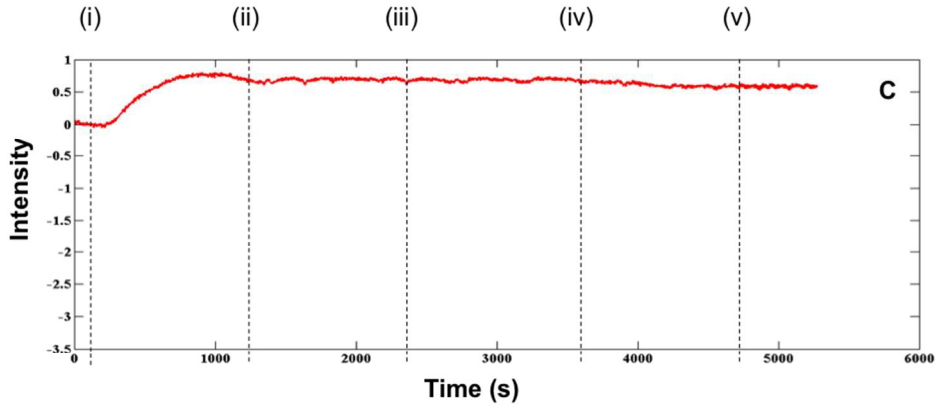

Figure 3

352x264mm (72 x 72 DPI)

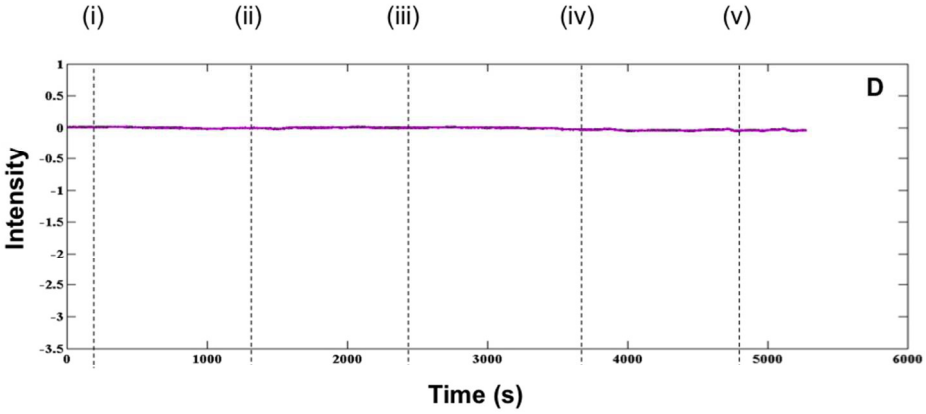

Figure 3

352x264mm (72 x 72 DPI)

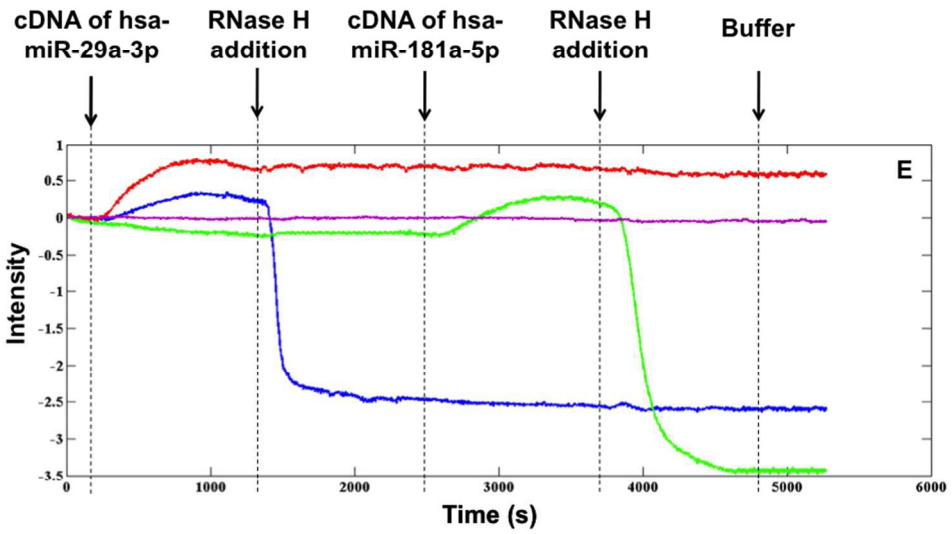

Figure 3

352x264mm (72 x 72 DPI)

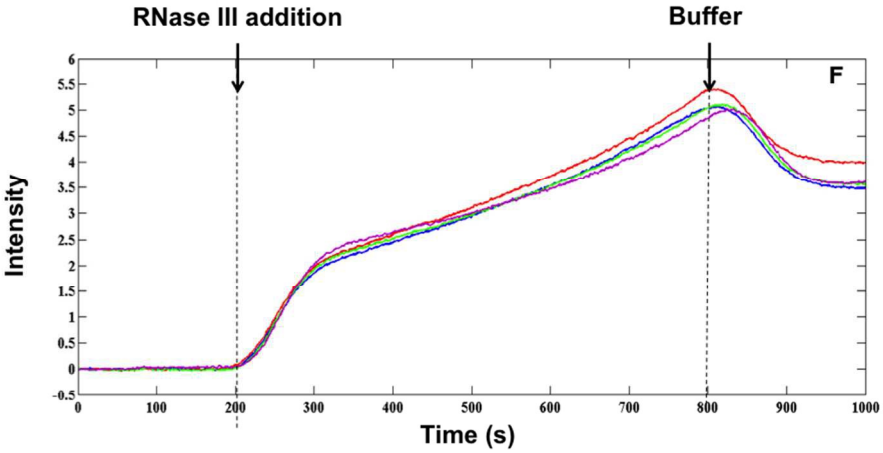

Figure 3

352x264mm (72 x 72 DPI)

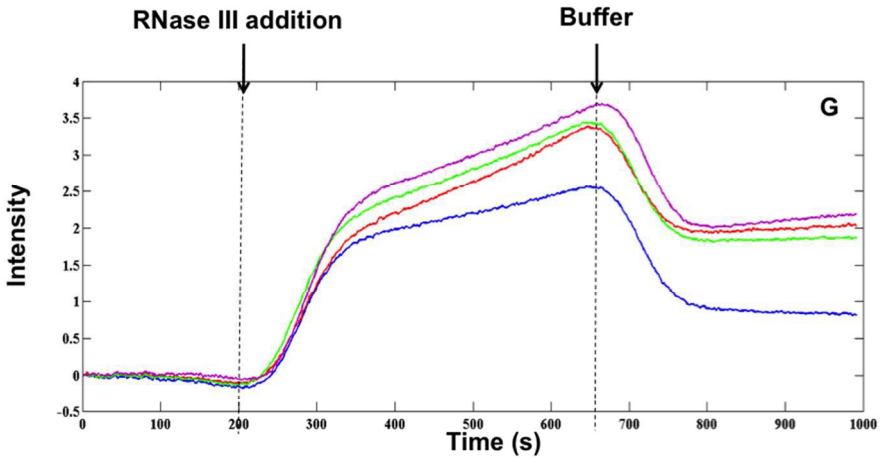

Figure 3

352x264mm (72 x 72 DPI)

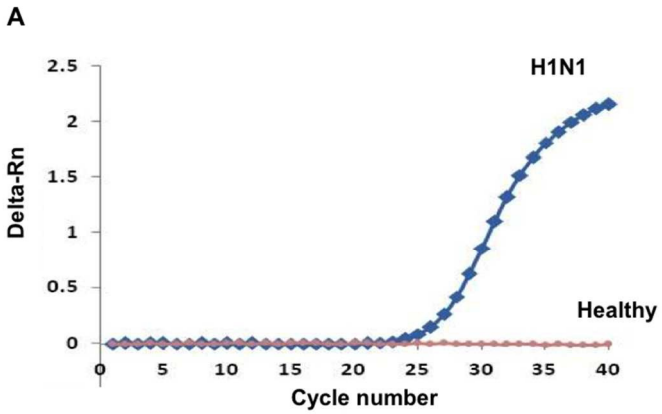

Figure 4

352x264mm (72 x 72 DPI)

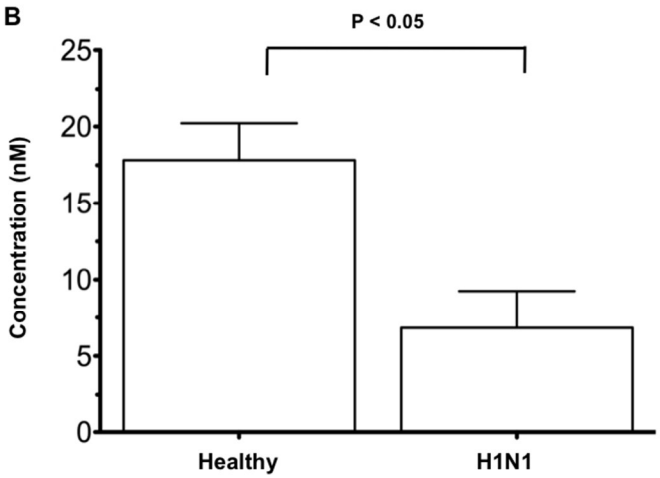

Figure 4

352x264mm (72 x 72 DPI)

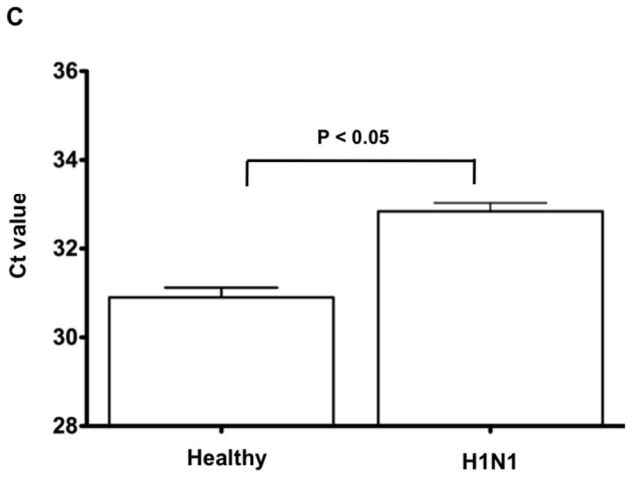

Figure 4

352x264mm (72 x 72 DPI)